Theory of Shock-Wave Ionization upon High-Velocity Impact of Micrometeorites

S. Drapatz and K. W. Michel

Max-Planck-Institut für Physik und Astrophysik, Institut für extraterrestrische Physik, Garching, Germany

(Z. Naturforsch. **29 a**, 870–879 [1974]; received March 21, 1974)

The relevant processes in shock wave ionization of a solid Fe micrometeorite impinging on a W target are analyzed. The internal energy behind the shock wave in shown to depend on impact velocity w, target and meteorite density in a simple analytical form. For low impact velocities ($w<7$ km sec^{-1}) the ions generated by the shock are mostly due to surface ionization. For high impact velocities ($w>20$ km sec^{-1}) the number of ions can satisfactorily be explained by isentropic expansion of the shocked material to a particle density of $n \approx 10^{20}$ cm^{-3} whereupon the rate processes in the expanding ion cloudlet govern the residual ionization. In velocity regions where laboratory measurements can be carried out, the agreement between theory and experiment confirms the assumptions made.

I. Introduction

Micrometeoroite detectors, residing on shock-wave ionization of fast interplanetary dust particles have successfully been used in satellite programs (HEOS-A2, PROSPERO) and are being developed for more elaborate studies in the future (HELIOS, MJS-Mission). In these experiments solid micrometeorites are partially evaporated and ionized upon high-velocity impact on a massive target plate. The ions, which are extracted by electric fields from the generated gas cloudlets, are recorded by detectors, possibly in conjunction with mass spectrometers [1]. The number and species of these ions are dependent on the size, the impact velocity w and the chemical composition of the micrometeorites. Upon impact, pressures and temperatures are reached which are not only of interest in astrophysics but also in a number of terrestrial applications (Figure 1). Shock wave ionization might offer an access to the equation of state at extreme pressures (above 100 Mbar), similarly as shock vaporization for the pressure range around 1 Mbar [2].

The relation between impact velocity, equation of state and shock wave entropy, and the relaxation phenomena in the unloading material are calculated in the following paper as a basis for the mass spectroscopic analysis of micrometeorites. We limit these considerations to the impact of Fe-particles onto a tungsten target, which has been investigated in the laboratory, and we try to describe the physical processes during the expansion of the material out of the impact crater (see Figure 2). A corresponding path-time diagram in the onedimensional approximation is shown in Fig. 3 (for particle properties: 1 μ diameter, $w = 5$ km sec^{-1}). At the moment of contact between particle and target, shock waves run into both materials, thereby heating them

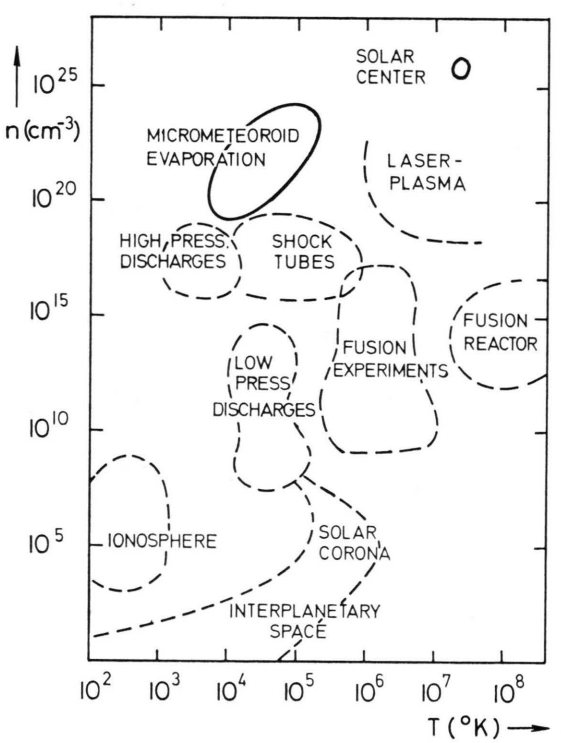

Fig. 1. Typical states of ionized gases in astrophysics and in the laboratory (after [21]), including the regime of micrometeoroite evaporation.

Reprint requests to Dr. K. Michel, Institut für Extraterrestr. Physik, MPI für Physik und Astrophysik, *D-8046 Garching*, bei München.

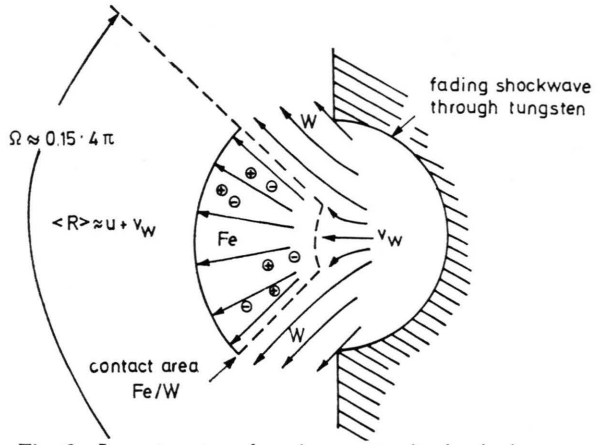

Fig. 2. Impact crater of an iron meteorite impinging on a tungsten target and expansion of the shocked material into vacuum.

effectively. When the shockfront arrives at the opposite free surface of the meteorite, rarefraction waves run back into the heated material. Thus the internal energy produced by the shock is converted into expansion energy or volume energy (V = specific volume) according to

$$\mathrm{d}E = -p\,\mathrm{d}V\,. \tag{1}$$

The important fact, however, is that this conversion is incomplete, i. e. the average expansion energy is only approximately equal to the specific energy behind the shock wave through the solid (u = particle velocity behind the shock [3, 4])

$$\Delta E_{\mathrm{H}} \gtrapprox \tfrac{1}{2}u^2$$

whereas the small remaining part is responsible for the residual ionization. To derive the relation between the initial properties of the impinging micrometeorite and the number and species of measured ions three major problems are to be solved:

(i) determine the state of matter behind the shock wave in dependence of impact velocity

(ii) calculate the remaining part of internal energy to find the temperature and the degree of ionization of the generated gas cloudlet

(iii) calculate the relaxation processes to determine the time, when the temperature and the corresponding degree of ionization is frozen in during the state of expansion.

II. State of Matter behind the Shock Wave

The starting point is the total internal energy behind the shock wave as a function of impact velocity w, where we have used laboratory [5] and atomic bomb [6] results for the region $w \lesssim 25\ \mathrm{km\ sec^{-1}}$ and the Thomas-Fermi-model [7] for velocities $w \gtrsim 50\ \mathrm{km\ sec^{-1}}$. The complete function $\Delta E_{\mathrm{H}}(w)$ is shown in Fig. 4, and it should be emphasized that beyond $w \gtrsim 10\ \mathrm{km\ sec^{-1}}$ this curve can quite accurately be represented by the approximation used for strong shocks [4]

$$\Delta E_{\mathrm{H}} = \frac{1}{2}\,u^2 = \frac{1}{2}\left(\frac{w}{\sqrt{\varrho_{\mathrm{Fe}}/\varrho_{\mathrm{w}}}+1}\right)^2 \approx 0.189\,w^2 \tag{2}$$

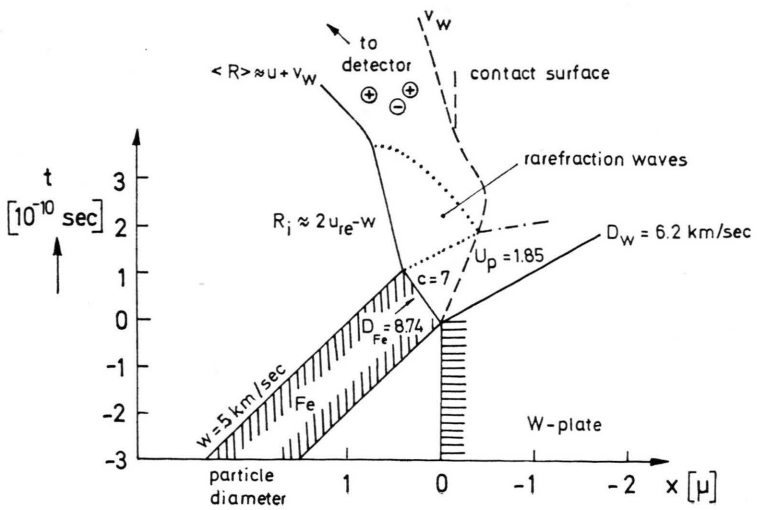

Fig. 3. Path time diagram of an iron particle impinging on a tungsten plate in one-dimensional approximation (particle properties: 1 μ diameter, impact velocity $w = 5\ \mathrm{km\ sec^{-1}}$). (meaning of symbols see App. A)

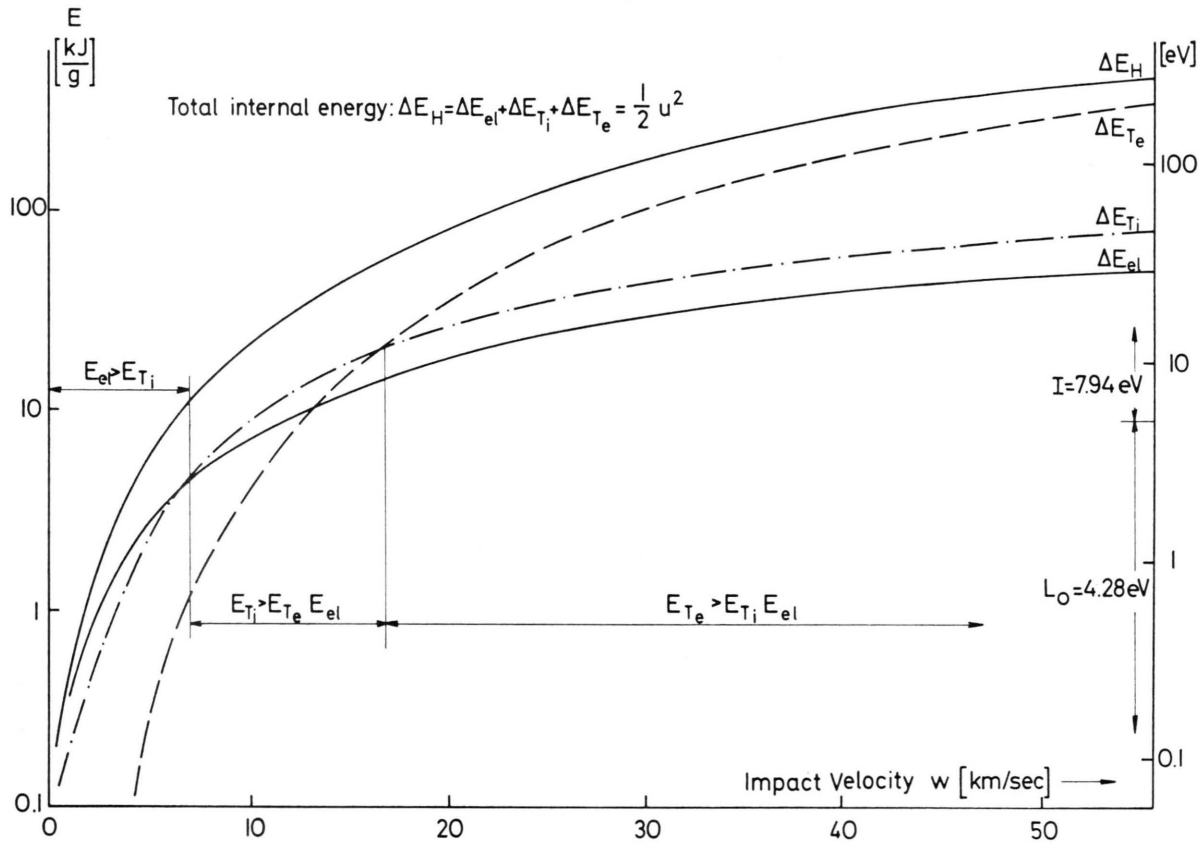

Fig. 4. The different contributions to the total energy ΔE_H behind a shock wave through Fe upon impact onto W at velocity w: elastic energy ΔE_{el}, thermal energy of nuclei ΔE_{Ti} and of electrons ΔE_{Te}.

where the only important properties of the material are the initial densities of W and Fe *. The derivation of Eq. (2) is given in Appendix A.

The total internal energy is a sum of three terms

$$\Delta E_H = \Delta E_{el} + \Delta E_{Ti} + \Delta E_{Te} \qquad (3)$$

where ΔE_{el} is caused by the elastic repulsion of the atoms in the lattice or liquid and ΔE_{Ti} and ΔE_{Te} by the vibrations of the nuclei and by electronic excitation, respectively. The different contributions in Eq. (3) have been determined from the Debye-temperature for the lattice and from a band model for the electrons. As seen in Fig. 4, the electronic excitation energy is approximately one order of magnitude higher than the other components for the high velocity region, but for $w \lesssim 10\,\mathrm{km\,sec^{-1}}$ the elastic energy is the dominant component. Here, in contrast to the high velocity regime, the energy is not sufficient for evaporation but only for fragmentation of the particle into smaller particles and the treatment of the problem turns out to be quite different for low and for high impact velocities.

* Equation (2) shows that the target material with the highest specific density should be chosen to obtain high energies in the impinging particle. Other considerations which govern the choice of the target include of course availability of high-purity materials in order to avoid target impurities in the expanding cloudlet (e. g. Au).

III. Treatment for Low Velocity Impact

In the low velocity case the impinging particle fragmentates into droplets with low temperatures ($T \lesssim 4000\,^\circ\mathrm{K}$). During the cooling time (10^{-7} sec) mainly impurities with low ionization potential will be ionized after diffusion to the surface from a depletion boundary layer. At an impact velocity of $6\,\mathrm{km\,sec^{-1}}$ the Fe particles are liquid, but the degree of vaporization does not exceed 5 per cent [2]. Thus, the generation of charged particles is dominated by impurities and does not represent the chemical composition of the meteorite directly.

All impurity atoms that can diffuse through liquid Fe to the surface during the evaporation cooling time τ may be evaporated. They are contained in a shell of thickness

$$\langle x \rangle = \sqrt{2\,D(T)\,\tau} \tag{4}$$

where the diffusion coefficient

$$D \approx 5 \cdot 10^{-5} \exp\{-5000/T\}\ \mathrm{cm^2\,sec^{-1}}$$

can be estimated from experiments with alkali metals in metals [8, 9].

The mass ΔM of iron atoms evaporated during time τ is given by the Hertz-Knudsen-equation

$$\Delta M/\tau = 4\pi r^2 \cdot P_S \sqrt{m/2\pi kT} = 6 \cdot 10^{-9} P_S \sqrt{m/2\pi kT} \tag{5}$$

where tables [10] for the iron vapor pressure P_S have been used. The ratio of ionized to neutral vapor atoms is obtained from the Saha-Langmuir-Equation for surface ionization

$$n_i/n_0 = (g_i/g_0) \exp[e(\Phi - I)/kT]\,. \tag{6}$$

The relevant quantities are

Φ: the work function of Fe (adequately modified to account for impurity atoms or electric fields [8]); I: the ionization potential of the evaporated material; g_0, g_i: statistical weights of atomic and ionic species.

Two examples of the calculated mass spectrum are shown in Fig. 5, where the Fe particle was assumed to contain 3 atom per cent of alkali metals and the ratio of alkali metals among one another as corresponding to the abundance in the earth's crust. The results agree well with laboratory experiments [1]. The main component Fe is not represented at all in the spectrum for impact velocities $w < 7\ \mathrm{km\,sec^{-1}}$.

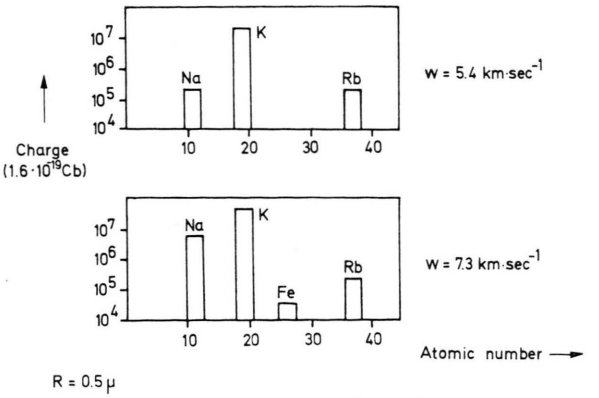

Fig. 5. Calculated mass spectrum of ions for an iron particle impinging on a W target at velocity w. The Fe particle was assumed to contain 3 atom per cent of alkali metals.

IV. Treatment for High-Velocity Impact

The treatment for high velocities is more difficult, since a complete evaporation takes place and the concept of an interface between a solid state and a vacuum is inapplicable. In the following, a pure iron meteorite is investigated to specify the conditions under which a substantial fraction of the material exists in the form of ions that do not recombine during expansion. The corresponding processes occurring in a hydrogen plasma have been discussed qualitatively by Kuznetzov and Raizer [11].

In order to solve Eq. (1) for E one needs the equation of state for the whole region of expansion, which is shown in Figure 6. For impact velocities of about 30 km sec^{-1} the Fe-particle is compressed by a factor of 3 and for this state fairly reliable solid

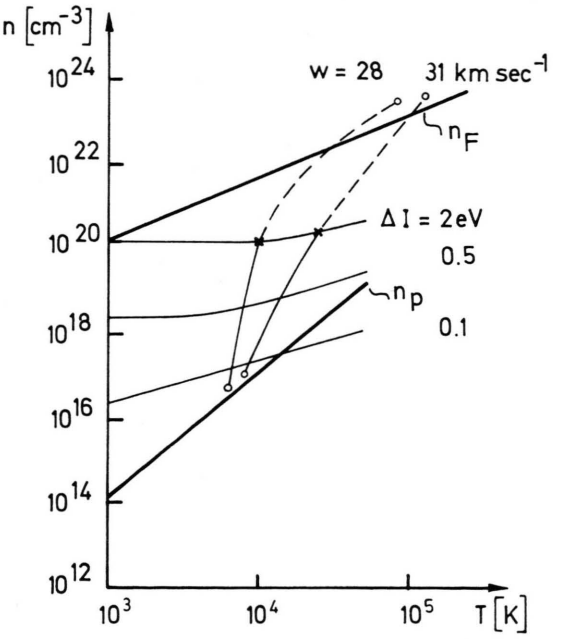

Fig. 6. Region of expansion of a shocked iron particle: n_F = Fermi limit, n_p = plasma limit [see Eq. (7)], ΔI = lowering of ionization potential [see Eq. (11)]. The dashed curve indicates quasistationary expansion, whereas the full line shows the region of relaxation.

state band models [12] are available. The non-equilibrium relaxation occurs in the low density part of the region shown, where the ideal gas law can be used with only slight corrections, e. g. for the lowering of the ionization potential [13]. At densities above the point where the ionization is frozen in, the densities are high enough for plasma effects to be negligible, since the particle distance is much

larger than the Debye length:

$$n^{-1/3} \gg (k\,T/4\,\pi\,n\,e^2)^{1/2}\,. \tag{7}$$

The whole expansion region of the material starting in the solid state phase and ending in the gaseous phase, thereby passing the Fermi limit and the critical region can only be described within a limited degree of accuracy by the following procedure. Equation (1) yields

$$(p\,\mathrm{d}V + \mathrm{d}E)/T = 0 = \mathrm{d}S \tag{8}$$

showing that the entropy for the solid state and the ideal gas phase are equal provided the temperature is a defined quantity, i. e. the relaxation along the dashed curves in Fig. 6 must be very fast for LTE to hold (see Appendix C). This might be the case for densities $n \gtrsim n_T = 10^{20}\,\mathrm{cm}^{-3}$, so that the residual ionization can be determined from the recombination rates in an ideal gas, which at $n \approx n_T$ has the same entropy as the compressed iron particle. The entropy at the high density part of the regime is calculated from the thermal energy of electrons (Fig. 4) and the electronic specific heat C_v given by the band-model.

$$\Delta E = \tfrac{1}{2}\,u^2 = \int_{T_0}^{T_s} C_v\,\mathrm{d}T\,,$$
$$S = \int_{0}^{T_s} C_v\,\mathrm{d}\ln T\,. \tag{9}$$

The result is equated to the entropy of an ideal gas in the low density part

$$S = (1-i)\,S_{\mathrm{F\,e}} + i\,(S_{\mathrm{F\,e}^+} + S_e) \tag{10}$$

with

$$\begin{aligned} S_j/k = {} & \tfrac{5}{2} - \ln n_j + \ln(2\,\pi\,m_j\,k\,T/h^2)^{3/2} \\ & + \ln \sum_\nu g_{j\nu} \exp\{-\varepsilon_{j\nu}/k\,T\} \\ & + 1/k\,T\,(\sum_\nu \varepsilon_{j\nu}\,g_{j\nu} \\ & \cdot \exp\{-\varepsilon_{j\nu}/k\,T\}/(\sum_\nu g_{j\nu} \exp\{-\varepsilon_{j\nu}/k\,T\}) \end{aligned}$$

in order to connect these two regions by the procedure of Equation (8). The equation for the gas entropy includes the thermal excitation of atoms and ions.

The corresponding degree of initial ionization is given by the Saha-Equation, where the lowering of the ionization limit ΔI has been taken into account

$$\frac{i^2}{1-i}\,n = \frac{2\,g^+}{g}\,\frac{(2\,\pi\,m_e\,k\,T)^{3/2}}{h^3} \exp\left\{-\frac{I_0 - \Delta I}{k\,T}\right\} = \frac{K}{n}\,,$$
$$\Delta I = (4\,\pi\,n\,e^6/k\,T)^{1/2} \quad \text{(Ref. [13])}. \tag{11}$$

Now, the material is expanding with approximately constant mean velocity u, where ion cores and electrons are thermally decoupled (Charge neutrality is conserved, however). Therefore, in the equation for conservation of energy we may deal with electron density n_e and electron temperature T_e only. With E_{in}^0 and E_{in}^+ being the internal excitation energy of atoms and ions, resp.

$$\begin{aligned} \frac{\mathrm{d}E_e}{\mathrm{d}t} &= -\,i\,k\,T_e\,\frac{\mathrm{d}\ln n_e}{\mathrm{d}t} \\ &= -\,\frac{p_e}{i}\,\frac{\mathrm{d}V}{\mathrm{d}t} - \frac{(I - E_{in}^0) + \frac{3}{2}k\,T_e}{i}\,\frac{\mathrm{d}i}{\mathrm{d}t} \\ &\quad + (1-i)\,\frac{\mathrm{d}E_{in}^0}{i\,\mathrm{d}T}\,\frac{\mathrm{d}T}{\mathrm{d}t} + \frac{\mathrm{d}E_{in}^+}{\mathrm{d}T}\,\frac{\mathrm{d}T}{\mathrm{d}t} \end{aligned} \tag{12}$$

with $$\frac{\mathrm{d}\ln n}{\mathrm{d}\ln t} = -3\,.$$

An electron gas is formed by free and bound electrons, which are coupled by two-body collisions. This gas is cooled by expansion [first term on right-hand side of Eq. (12)] and heated by recombination and deexcitation of electrons. Although the mean free path of electrons exceeds the dimension of the ion cloudlet, the electrons near the edge of the cloudlet are deflected by an electrostatic potential. This potential wall has been built up by some electrons that have escaped the cloudlet. Thus, one can write a conventional ansatz for the equation describing the most important relaxation process, namely the three-body recombination, using a recombination coefficient α.

$$\begin{aligned} \mathrm{d}i/\mathrm{d}t = {} & -\,\alpha\,i\,n\,(i^2\,n - (1-i)\,K) \\ & \text{with } \alpha = \alpha_0\,T^{-9/2} \text{ (Ref. [14])}\,. \end{aligned} \tag{13}$$

The reverse reaction, collisional ionization, is allowed for by microscopic reversibility (equilibrium constant K). Numerical calculations have been carried out to solve the system of Equations (12) and (13).

In order to present the conditions during expansion in one picture, the term "freezing point" in Fig. 7 has been used in the sense that beyond this region the degree of ionization will not drop by more than $\approx 10\%$ to the asymptotic value. In Appendix B it is shown that this asymptotic value differs substantially from zero.

The numerical calculations show (Fig. 7) that even for larger particles (number of atoms $N \gtrsim 10^9$) the freezing point occurs at $t < 10^{-9}$ sec, so that cooling by radiation of visible light is negligible.

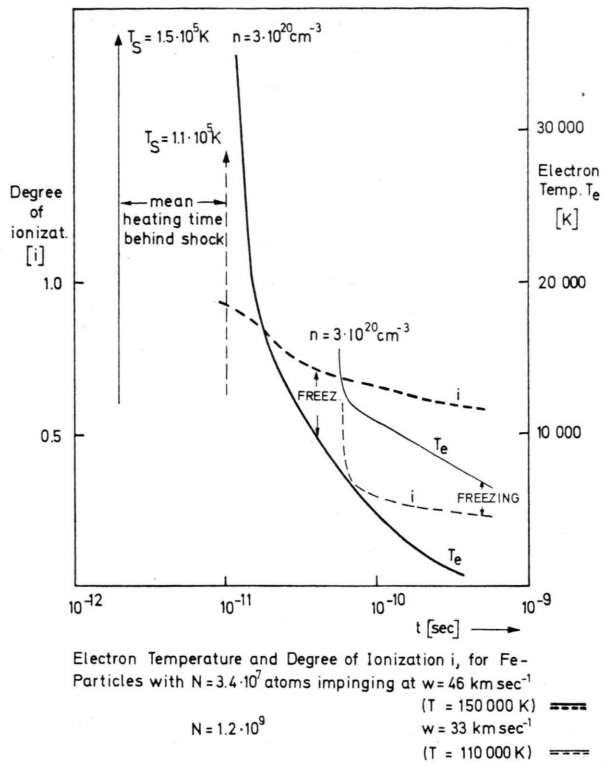

Fig. 7. Time scale of relaxation in the unloading material, which is generated by impinging Fe-particles of different masses and velocities. The term "freezing point" has been used in the sense that beyond this region the degree of ionization will not drop by more than $\approx 10\%$ to the asymptotic value.

On the other hand the calculations fail for particles with $N \lesssim 10^7$, because the corresponding expansion time $t \lesssim 10^{-11}$ sec is too small for LTE to hold (see Appendix C).

A summary of the calculations is displayed in Fig. 8: the residual ionization i_R as a function of impact velocity for a larger and a smaller particle. Two interesting conclusions are: (i) for velocities $w \gtrsim 40$ km sec^{-1} the residual ionization is independent of the particle size, as long as this size is within the limits of the model, (ii) for velocities below 15 km sec^{-1} – depending on the particle size – the residual ionization is not determined by volume ionization but by surface ionization as mentioned above (Section III).

V. Summary and Conclusion

As a basis for the mass spectroscopic analysis of micrometeorites the relation between impact velocity, equation of state and shock wave entropy as well as the relaxation phenomena in the unloading material have been investigated.

For the low velocity region ($w < 10$ km sec^{-1}) the production of charged particles is dominated by the impurities with the lowest ionization potential. Especially alkali metals, present only as trace elements in the micro-meteorite, form the major component in the mass spectrum. This is in good agreement with measurements [1].

For the high velocity region ($w > 20$ km sec^{-1}), it has tacitly been taken for granted without specification of the relaxation processes, that the expansion of the ion cloud proceeds isentropically down to densities of $n \approx 10^{20}$ cm^{-3} on time scales as short as 10^{-9} secs. The good agreement of these computational results with experimental measurements available [1], corroborates this assumption. A

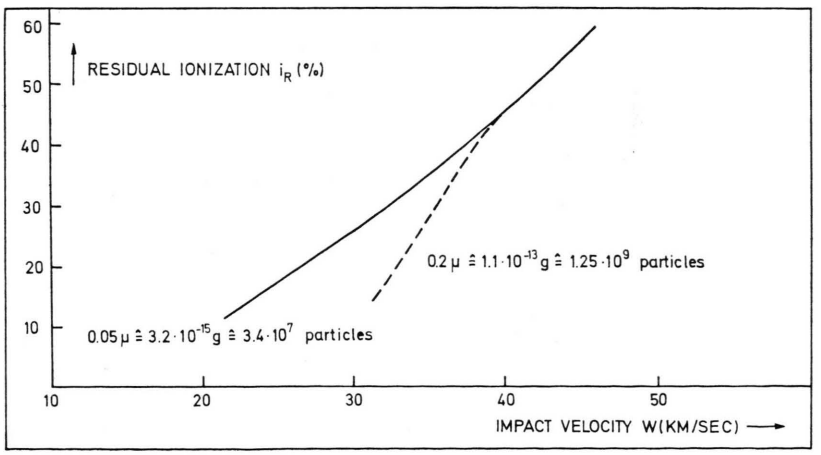

Fig. 8. Calculated residual ionization as a function of impact velocity for Fe-particles of different mass.

severe theoretical justification, however, is not possible at present because relaxation processes in solids (not to speak of the transition region between solid and gas) are badly understood. Progress in this field should be possible from two different aspects: starting with relaxation in solid states using the exciton concept on the one side or starting with molecular relaxation and using the autoionization concept on the other.

The results of our calculation for the high (Fig. 8) and low (Fig. 5) velocity cases are summarized in Fig. 9 under the assumption that the number of charged particles collected by the detector is proportional to the mass of the impinging particle. This relation holds for low velocities, since the micrometeorite will fragmentate into a higher number of particles and for higher velocities, where complete evaporation takes place. For $w > 20$ km sec^{-1} the impinging micrometeorite is evaporated completely and the mass spectrum shows the real chemical composition of the particle. A small portion of impurities ($< 10^{-5}$) is completely negligible. For velocities $w > 40$ km sec^{-1} the residual ionization is independent of the particle size.

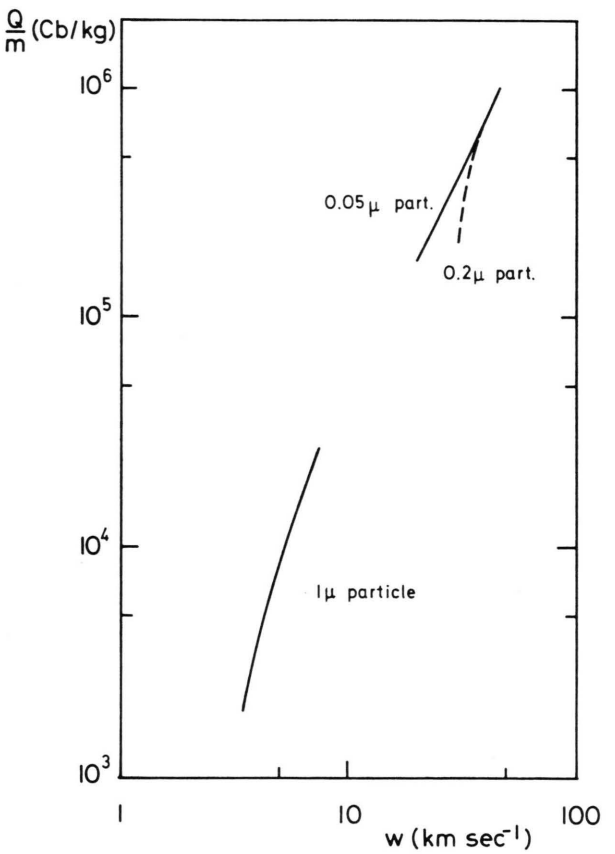

Fig. 9. Summary of the calculations in the high-temperature and low-temperature regime: yield of ions as a function of impact velocity (see Fig. 5 and Fig. 9 for reference).

Acknowledgements

We are grateful to K. Hornung for the numerical calculation of the shock wave entropy of Fe. Valuable discussion with H. Fechtig and H. Dietzel (Max-Planck-Institut Heidelberg) are gratefully acknowledged.

Appendix A

It is convenient to represent laboratory measurements on solid state shock waves by a linear relation between shock wave velocity D and flow velocity u behind the shock wave

$$D = A + B\,u\,. \tag{A 1}$$

These so-called Hugoniot relationships (for Fe and the target material W) together with the condition that pressures and flow velocities have to be equal on both sides of the contact surface, namely

$$\begin{aligned} P_{\mathrm{Fe}} &= P_{\mathrm{w}}\,, \\ w - u_{\mathrm{Fe}} &= u_{\mathrm{w}}\,, \\ P &= \varrho\, D\, u \end{aligned} \tag{A 2}$$

(ϱ = density in front of the shock wave),

provide an analytic relation between the flow velocity u in Fe behind the shock wave and the impact velocity w. Since

$$\Delta E_{\mathrm{H}} = \tfrac{1}{2}\,u^2 \tag{A 3}$$

the total internal energy is given by w and the experimental values discussed before. For strong shocks $B \cdot u \gg A$ in Eq. (A 1) and the Grüneisen-Parameter $\Gamma = 2(B-1)$.

Thus

$$D = \tfrac{1}{2}(\Gamma + 2)\,u \tag{A 4}$$

and using the conditions at the contact surface (A 2) one obtains

$$u = \left(\sqrt{\frac{\varrho_{\mathrm{Fe}}}{\varrho_{\mathrm{w}}} \frac{\Gamma_{\mathrm{Fe}} + 2}{\Gamma_{\mathrm{w}} + 2}} + 1 \right)^{-1} w\,. \tag{A 5}$$

Since in the limit of the Thomas-Fermi-model [2] the Grüneisen-Parameter is the same for all materials, i. e. $\Gamma_{\mathrm{Fe}} \approx \Gamma_{\mathrm{W}}$, one obtains for strong shocks

$$u = w/(\sqrt{\varrho_{\mathrm{Fe}}/\varrho_{\mathrm{w}}} + 1) = 0.615\,w \tag{A 6}$$

and for the internal energy

$$\Delta E = \tfrac{1}{2}\, u^2 = 0.189\, w^2 \text{ per gramm}\,. \qquad \text{(A 7)}$$

This simple relationship, that should only be valid for $w > 50$ km sec^{-1}, turns out to be a good analytical approximation of the experimental Hugoniot curve down to impact velocities $w \lesssim 10$ km sec^{-1}.

Appendix B

We show by a lower limit estimate that the system of Eqs. (12) and (13) has a non-vanishing asymptotic solution for the degree of residual ionization i_R. A similar investigation has been carried out for low expansion velocities and low initial degree of ionization by Kuznetzov and Raizer [11]. Neglecting the ionization term in Eq. (13) one obtains

$$\mathrm{d}i/\mathrm{d}t = -\,a_0\, n^2\, i^3/T^{9/2}\,. \qquad \text{(A 8)}$$

Using

$$x = -\,\mathrm{d}\ln i/\mathrm{d}\ln t \qquad \text{(A 9)}$$

and spherically symmetric expansion at constant mean velocity u

$$\mathrm{d}\ln n/\mathrm{d}\ln t = -3$$

one has

$$-\,\mathrm{d}\ln x/\mathrm{d}\ln t = 5 + 2\,x + \tfrac{9}{2}\,\mathrm{d}\ln T/\mathrm{d}\ln t\,. \qquad \text{(A 10)}$$

Neglecting the excitation energy of atoms and ions in equation (12) one obtains

$$\frac{\mathrm{d}\ln T}{\mathrm{d}\ln t} = -2 + \left(-\frac{2}{3}\,\frac{I}{kT}\,\frac{\mathrm{d}\ln i}{\mathrm{d}\ln t}\right) - \frac{\mathrm{d}\ln i}{\mathrm{d}\ln t} = -2 + y + x$$

with $$\ln y = \ln\left(\frac{2\,I}{3\,k}\right) - \ln T + \ln x\,. \qquad \text{(A 11)}$$

Combining Eq. (A 9), (A 10), and (A 11) yields

$$\frac{\mathrm{d}\ln y}{\mathrm{d}\ln x} = \frac{11\,y + 15\,x - 12}{9\,y + 13\,x - 8}\,. \qquad \text{(A 12)}$$

The solutions of Eq. (A 12) are displayed schematically in Fig. 10 (with nodes [0, 0] and [0, 12/11] and one saddle point [8/13, 0]). Since the solutions converge at the point $x = 0$, $y = 12/11$, one obtains as asymptotic values

$$i_R \to \text{const} \quad \text{(from A 9)}\,,$$
$$T \sim t^{-10/11} \quad \text{(from A 11)}\,. \qquad \text{(A 13)}$$

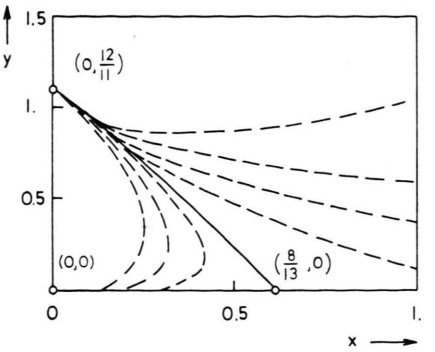

Fig. 10. Solution of Eq. (A 12) which gives a lower limit estimate for the residual ionization (see text).

Appendix C

In order to connect the high density and low density region by equating the entropies of both states [Eq. (8)] LTE must exist in the transient ionized gas (along the dashed lines in Figure 6). A corresponding rough criterion for the relaxation time scale in dependence of expansion velocity v and particle dimensions R is given by

$$\tau \ll R/v \approx 10^{-9}\,\text{secs}\,.$$

Here, we present arguments showing that this criterion might be fulfilled at least in the two limiting cases, in the high density and in the low density case. Since in both cases we are well above the plasma limit, collective plasma effects are considered to be negligible and single particle effects will be investigated.

In the high density region the ion cores are heated immediately by the shock and the heat is transferred to the electrons. For densities as high as 10^{23} cm^{-3} and comparatively low temperatures of 10^5 °K the diffusion theory for equipartition of energy in ionized gases [15] breaks down. A rough but adequate picture is given by nonadiabatic collisions between heavy particles where considerable progress has been made in the last decade [16]. Different authors have investigated the energy spectra of the electrons emitted upon ionization by these collisions based on an analysis of the transition from discrete terms of a generated quasi-molecule to the continuous spectrum. These autoionizing states will be deexcited by radiationless transitions fast enough ($\tau \approx 10^{-12} - 10^{-15}$ sec) in order to heat the electron gas during expansion.

For lower densities (perfect gas regime) fast three body collisions establish equilibrium in the electron gas. After an electron has been transferred to an excited state of the Fe-atom

$$Fe^+ + e + e \rightarrow Fe^* + e$$

this state may then be transferred to higher or lower levels or reionized by inelastic electron collisions. The fraction of excited atoms ending up in the ground state constitutes the recombination. Thus the relaxation time scale is given by the time scales for ionization and de-excitation by electron collisions. Radiative optical transitions cannot compete in the state of rapid expansion. Collisional transition probabilities for Fe in the interesting region ($n_e \approx 10^{19}\,cm^{-3}$, $T = 10^4\,°K$) are given in Fig. 11: ionization probabilities calculated using an empirical formula [17], de-excitation probabilities calculated from f-value measurements [18] using the effective Gaunt factor formula [19] and from measurements of excitation cross sections [20]. The corresponding cross-sections for hydrogen (at distorted energy scale) are given for comparison. As seen in the figure, all relaxation time scales are shorter ($\tau \approx 10^{-9} - 10^{-12}$ secs) than the expansion time scale. But it should be kept in mind that the complete recombination to the ground state requires several de-excitation transitions.

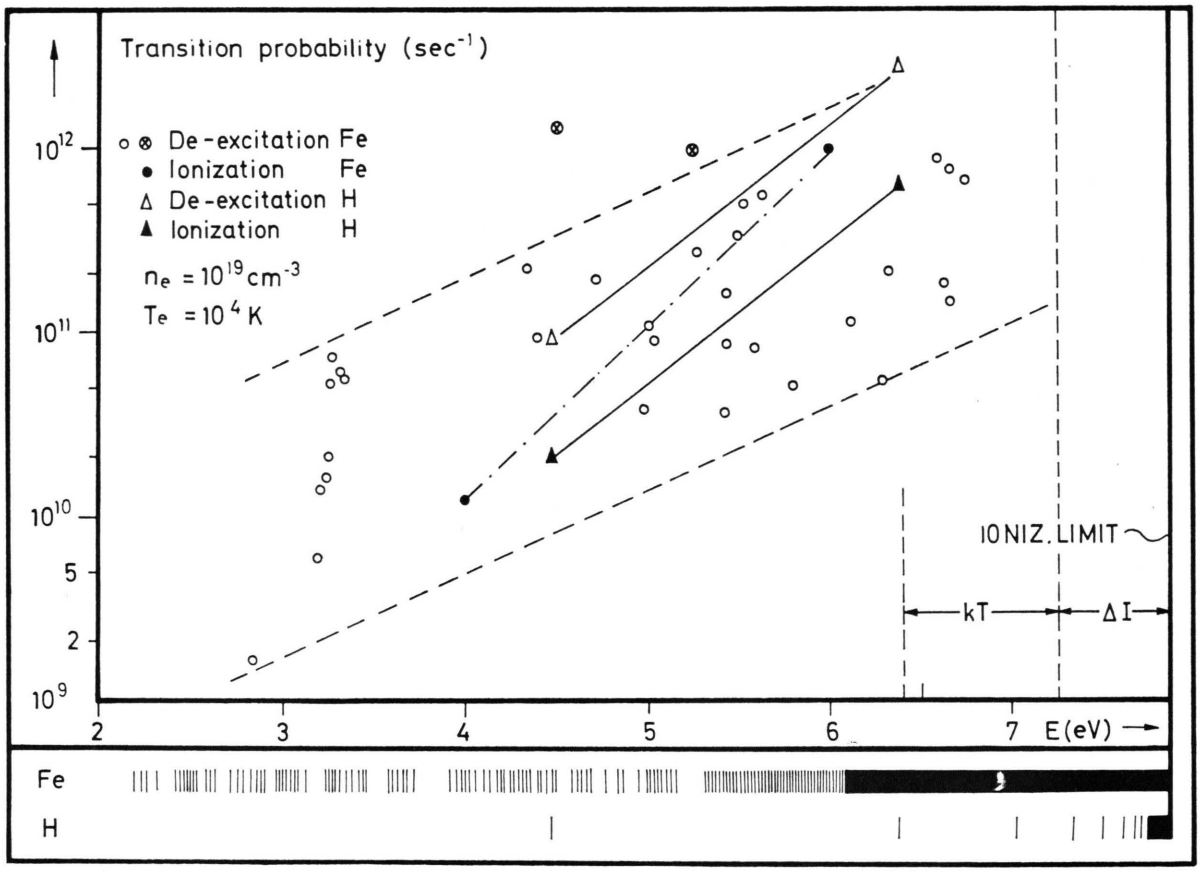

Fig. 11. Transition rates of Fe-atoms under typical conditions of the relaxation regime (for details see text). Note that time scales considered here lie in the range $10^{-9} - 10^{-12}$ sec.

[1] P. Rauser and H. Fechtig, Space Res. XII, 391 [1972].
[2] K. Hornung and K.-W. Michel, J. Chem. Phys. **56**, 2072 [1972].
[3] K.-W. Michel and H. G. Wagner, Naturwiss. **58**, 65 [1971].
[4] Yu. Zel'dovich and P. Raizer, Physics of Shock Waves and High-Temperature Hydrodynamic Phenomena. Academic Press, New York 1967.
[5] M. van Thiel et al., Compendium on Shock Wave Data. UCRL-Report, UCRL-50, 108 [1966–67].
[6] L. V. Al'tshuler et al., Sov. Phys. JETP **27**, 420 [1968].
[7] W. Geiger, H. Hornberg, and K. H. Schramm, Springer Tracts in Modern Physics **46**, 1 [1968].
[8] M. Kaminsky, Atomic and Ionic Impact Phenomena on Metal Surfaces, Springer-Verlag, Berlin 1965.

[9] R. C. L. Bothworth, Proc. Roy. Soc. London A **150,** 58 [1935].
[10] R. Hultgren, R. L. Orr, P. D. Anderson, and K. K. Kelley, Selected values of Thermodyn. Properties of Metals and Alloys. Wiley, New York 1963.
[11] N. M. Kuznetsov and Yu. Raizer, Zh. Prikl. Mekh. Tekh. Fiz. **4,** 10 [1965].
[12] G. M. Gandel'man, Sov. Phys. JETP **24,** 99 [1967].
[13] G. Ecker and W. Kröll, Erniedrigung der Ionisierungsenergie in einem Plasma. Forschungsberichte Nordrhein-westf. **1962,** 1221.
[14] B. Makin and J. C. Keck, Phys. Rev. Lett. **11,** 281 [1963].
[15] L. Spitzer, Physics of Fully Ionized Gases, Interscience, New York 1956.
[16] G. N. Ogurtsov, Rev. Mod. Phys. **44,** 1 [1972].
[17] W. Lotz, Z. Phys. **206,** 207 [1967].
[18] T. Garz and M. Kock, Astr. Astroph. **2,** 274 [1969].
[19] H. v. Regemorter, Astrophys. J. **136,** 906 [1962].
[20] I. M. Belousova and D. B. Gurevich, Opt. Spectrosc. **10,** 206 [1961].
[21] P. Mulser, R. Sigel, and S. Witkowski, Phys. Rep. (Phys. Lett. C) **6,** 187 [1973].